

RESEARCH ARTICLE

Thoracic radiography of healthy captive male and female Squirrel monkey (*Saimiri* spp.)

Blandine Houdellier¹*, Véronique Liekens², Pascale Smets², Tim Bouts³, Jimmy H. Saunders¹

1 Department of Medical Imaging and Small Animal Orthopaedic, Faculty of Veterinary Medicine, Gent University, Merelbeke, Belgium, **2** Department of Small Animal Medicine, Faculty of Veterinary Medicine, Gent University, Merelbeke, Belgium, **3** Zoo of Pairi Daiza, Brugelette, Belgium

* These authors contributed equally to this work.

* blandine.houdellier@gmail.com



OPEN ACCESS

Citation: Houdellier B, Liekens V, Smets P, Bouts T, Saunders JH (2018) Thoracic radiography of healthy captive male and female Squirrel monkey (*Saimiri* spp.). PLoS ONE 13(8): e0201646. <https://doi.org/10.1371/journal.pone.0201646>

Editor: Katja N. Koeppel, University of Pretoria, SOUTH AFRICA

Received: September 24, 2017

Accepted: July 19, 2018

Published: August 7, 2018

Copyright: © 2018 Houdellier et al. This is an open access article distributed under the terms of the [Creative Commons Attribution License](https://creativecommons.org/licenses/by/4.0/), which permits unrestricted use, distribution, and reproduction in any medium, provided the original author and source are credited.

Data Availability Statement: All relevant data are within the paper and its supporting information files.

Funding: The authors received no specific funding for this work. Tim Bouts is an independent practitioner affiliated to, but not funded by, Zoo of Pairi Daiza, Brugelette, Belgium. Zoo of Pairi Daiza did not have a role in the study design, data collection and analysis, decision to publish, or preparation of the manuscript. The specific role of this author is articulated in the 'author contributions' section.

Abstract

The purpose of this prospective study was to describe the normal anatomy and provide reference ranges for measurements of thoracic radiography on Squirrel monkeys (n = 13). Thoracic radiography is a common non-invasive diagnostic tool for both cardiac and non-cardiac thoracic structures. Furthermore cardiac disease is a common condition in captive primates. In this study, left-right lateral, right-left lateral and dorsoventral projections of 13 healthy Squirrel monkeys were reviewed during their annual health examinations. The mean Vertebral Heart Score on the left-right and right-left lateral projections were $8,98 \pm 0,25$ and $8,85 \pm 0,35$ respectively. The cardio-thoracic ratio on the dorsoventral projection was $0,68 \pm 0,03$. The trachea to inlet ratio was $0,33 \pm 0,04$. Other measurements are provided for the skeletal, cardiac and respiratory systems. Knowledge of the normal radiographic thoracic anatomy is fundamental in clinical as well as research settings for accurate diagnosis of diseases.

Introduction

Squirrel monkeys are arboreal neotropical monkeys, belonging to the family of Cebidae and subfamily Saimirinae. Many genetic sequence data have been obtained from the currently organized squirrel monkey taxa: *S. oerstedii oerstedii*, *S. o. citronellus*, *S. cassiquiarensis cassiquiarensis*, *S. c. albigena*, *S. macrodon*, *S. ustus*, *S. sciureus sciureus*, *S. s. collinsi*, *S. boliviensis boliviensis*, *S. b. peruviansis*, and *S. vanzolinii* [1].

Squirrel monkeys are useful animal models in a variety of different disciplines in biomedical research due to their phylogenetic similarities to humans [2]. Many studies have been published in order to better understand the basic biology [2–5], biogeography [3, 6], morphology [2, 3, 5–8] and also behavior [2, 9, 10] of this species. However, research has still to be done to better understand the biology and morphology of this species.

Cardiovascular diseases are particularly overrepresented in monkeys, having been identified as a major cause of death in squirrel monkeys particularly [11], in other primates [12] and captive great apes [13]. Reviews of mortality report that cardiovascular diseases represent 41% of deaths in gorillas [14], and 81,25% in aged chimpanzee [15]. Cases of dilated (DCM) and

Competing interests: The examinations were done in the zoo of Pairi Daiza as part of the annual health examination. The zoo of Pairi Daiza paid for the blood sample analysis and provided the radiography machine (present on site). There are no patents, products in development or marketed products to declare. This does not alter our adherence to PLOS ONE policies on sharing data and materials.

hypertrophic cardiomyopathy (HCM) like phenotype have been reported in aged Squirrel monkeys [11, 16]. High prevalence of DCM has also been demonstrated in other small monkeys [12, 17]. Multiple reviews of fibrosing cardiomyopathy are reported in multiple species [17–21] and a strong genetic predisposition in Rhesus macaques (*Macaca Mulatta*) for HCM has been demonstrated [22].

Because of the importance of cardiac disease in this species, previous research concentrated on electrocardiographic and echocardiographic characteristics of Squirrel monkeys [23]. Some publications are also available on smaller monkeys like Francois Langurs (*Trachypithecus francoisi*) [17]. Echocardiography may be the preferred examination for cardiac disease, but thoracic radiography is a quicker and easier examination that can give a lot of basic information on both cardiac and non-cardiac thoracic structures. Thoracic radiography is essential to access lower airway disease and is commonly used in non-human primates. The radiographic thoracic anatomy has been studied in many other more or less similar species like ring-tailed lemur (*Lemur catta*) [24], Goeldi's monkey (*Callimico goeldi*) [25], Rhesus macaque [26], Cynomolgus monkey (*Macaca fascicularis*) [27], pet macaques of Sulawesi (*Macaca nigra* and *tonkeana*) [28], vervet monkey (*Chlorocebus sabaeus*) [29] and also in close species as in capuchin (*Cebus paella*) [30]. The tracheal morphology has also been studied in *Saimiri* spp. [31]. Lower airway disease has been reported as viral and bacterial infection in chimpanzees and macaques [32]. Toxoplasmosis has been reported in squirrel monkeys [33, 34] and bronchopneumonia has been demonstrated to be the most frequent cause of death in older animals [35].

The aim of this study is to describe the normal radiographic thoracic anatomy of the *Saimiri* spp. as a species-specific reference.

Materials and methods

All examinations were performed on site in the veterinary hospital (Pairi Daiza, Brugelette, Belgium). The data used in the study were collected during the annual health examination, that includes physical examination, blood sampling, radiography of the thorax and echocardiography, of the animals.

Animals

Fourteen captive Squirrel monkeys (*Saimiri* spp.), 9 *Saimiri boliviensis peruviansis* and 5 *Saimiri sciureus*, from Pairi Daiza, Belgium were submitted for a full clinical examination including cardiac biomarkers (N Terminal-prohormone of Brain Natriuretic peptide “NT-proBNP” and troponin I, tests performed by Electrochemiluminescence “ECLIA”) and complete echocardiographic examination performed by a board-certified cardiologist for evaluation of the cardiovascular system (PS). One *Saimiri boliviensis peruviansis* presented a significant abnormality (severe dilation of the ascending aorta) on echocardiography and was excluded from the study. The remaining 13 monkeys were included in the study.

The age of the animals ranged from 2,25 to 21,3 years (mean age = 9,12 years). The minimum and maximum weights of the animals were 467 g and 756 g respectively (mean weight = 615 g). There were 11 females and 2 males. All 14 animals are housed in a combined indoor (200 square meters) and outdoor (islands of 1360 and 1650 square metres) enclosure with multiple environmental enrichments such as ropes and sticks. The environment is natural with trees and plants, and their food is based on fruits, vegetables and primates diet (MAZURI®).

This study adhered to the legal requirements of Belgium and is in accordance with the recommendations of the Weatherall report on the use of non-human primates.

Anaesthesia

No animals were anesthetized for any other reasons than their general health examinations.

Examinations were performed under general anaesthesia. Induction and maintenance of anaesthesia was by mask. An Ayre's T-piece was used for all animals to minimize resistance and dead space. The volume of oxygen was kept at 2 L/min at all times and the percentage of isoflurane (Isoflo, Eucuphar) varied depending on the anaesthetic monitoring of the patient. The percentage was on the maximum value (5%) for induction and was slowly decreased until 1,5–2% for maintenance. During the entire anaesthesia, heart rate and oxygen saturation was monitored by pulse-oxymetry placed on the hand, respiratory rate was counted manually and rectal temperature was continuously monitored with a digital probe. Anaesthetic depth was monitored by checking eyelid (medial palpebral reflex) and cornea reflexes. Individual anaesthetic files were kept for all animals. Due to the small size of the animals, maintaining the temperature was the main challenge. Plastic gloves filled with hot water (37°C), a heating carpet (38°C) as well as pre-heated sonographic gel were used. All animals received 20 mL of saline solution (Ringer Lactate[®] solution) subcutaneously at the beginning of anaesthesia. After anaesthesia, animals were allowed to recover in a small dark transport cage in a heated room before being transported back to their enclosure. Animals were monitored after anaesthesia for 3 days without adverse effects.

After radiographic examinations, all animals underwent a complete echocardiographic examination by a board-certified cardiologist and an electrocardiogram (ECG) with the AliveCor system (Veterinary iPhone[®] ECG and heart monitor). The minimum and maximum time of anesthesia were 22 minutes and 35 minutes respectively (mean time = 31 minutes).

Radiography

Left-right lateral (RL), right-left lateral (LL) and Dorsoventral (DV) radiographic projections of the thorax were taken at the end of inspiration using a direct digital radiography device (Sound-Eklin[®]). On one animal (*Saimiri boliviensis peruviansis*), the head was superimposed with the cranial aspect of the thoracic cavity on the DV projection due to the short neck conformation. On one patient, a straight DV projection could not be performed. The Source to Image Distance (SID) was settled at 100 cm and images were obtained with 60 kVp and 2,5 mAs. The radiographs were stored in DICOM format and were archived to a PACS system.

Criteria for interpretation

All the radiographic images were analyzed by the same observer (BH), that evaluated all the thoracic structures individually.

- The presence or absence of a clavicle was recorded.
- The number of ribs (including floating ribs), vertebrae (including the anticlinal vertebra) and sternbrae were recorded. The length and height of the vertebrae and sternbrae were measured on the RL projection from the midpoint of the cranial end plate to the caudal end plate (length) (Fig 1) and along the cranial endplates (height) [24].
- The tracheal diameter and more precisely the trachea to thoracic inlet ratio was calculated as proposed in dogs and monkeys [24, 36]. The tracheal inclination was calculated as the angle formed by the ventral surface of the bodies of the thoracic vertebrae and the trachea [30]. The location of the carina was also defined (Fig 2).
- For evaluation of the cardiac size, the ratio of the cardiac height/thoracic height on the lateral projections, as well as the width on the DV projection (at the widest point of the cardiac

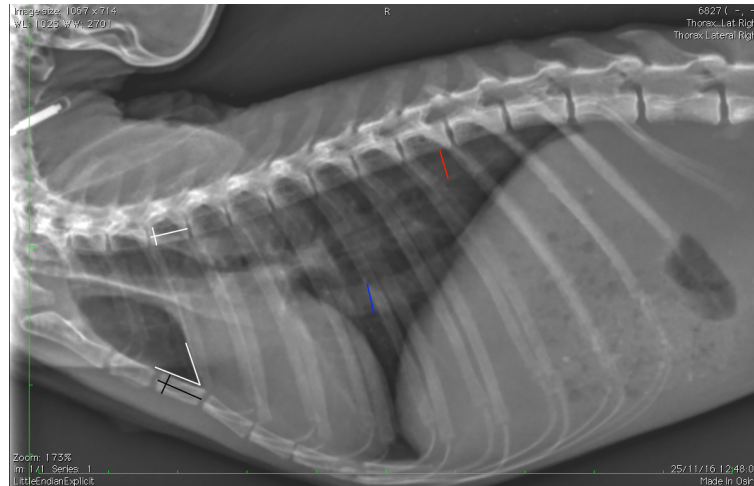


Fig 1. Left-right lateral projection of a 9 years old *Saimiri sciureus* showing the measurements of the length and height of the thoracic vertebrae (white lines) and sternbrae (black lines). The diameter of the aorta (red line) and caudal vena cava (blue line) are also presented. The angle of cardiac inclination is represented by the two white lines between the cranial border of the cardiac silhouette and the sternbrae.

<https://doi.org/10.1371/journal.pone.0201646.g001>

silhouette) have been calculated (Fig 3). The number of intercostal space occupied by the cardiac silhouette has also been reported in order to have multiple measurements available and to be more accurate.

- The angle of cardiac inclination is formed by the right cardiac border and the sternum on the lateral projection as described [24, 30, 37] (Fig 1). The number of sternbrae in contact with the cardiac silhouette has also been calculated.
- The Vertebral Heart Score (VHS) was measured on the RL (RL-VHS) and LL (LL-VHS) projections according to the protocol established in dogs [38] (Fig 4).

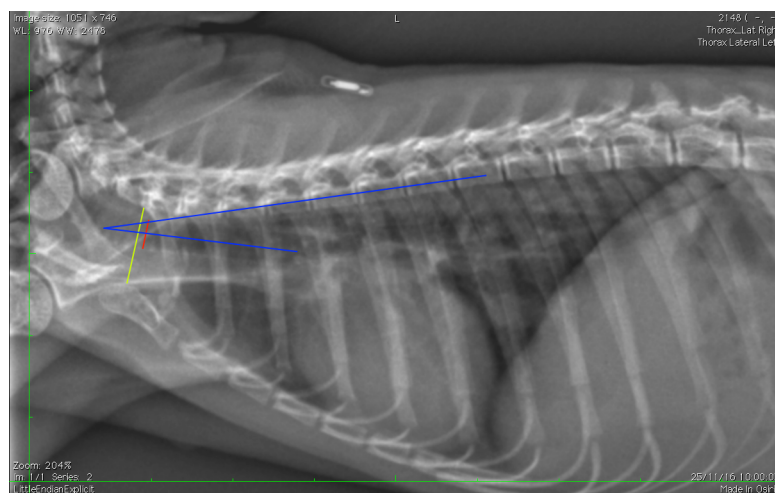


Fig 2. Right-left lateral projection of a 4 year old *Saimiri boliviensis peruvienis*. Measurements of tracheal diameter (red line) to thoracic inlet length (yellow line) ratio; tracheal inclination (blue lines) are presented. Note the carina located at the level of the third intercostal space.

<https://doi.org/10.1371/journal.pone.0201646.g002>

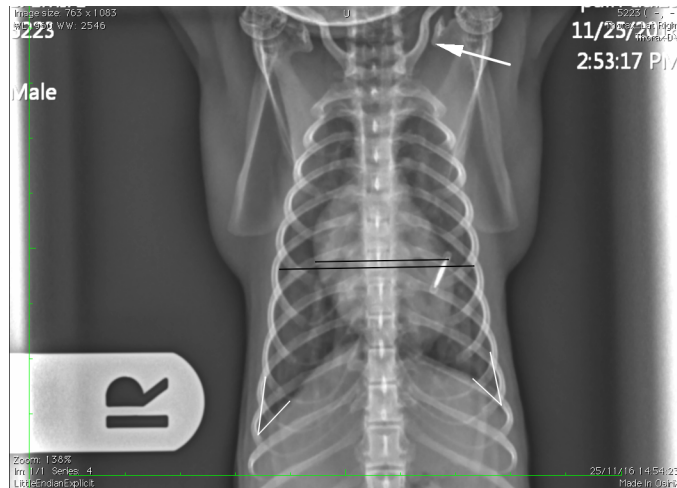


Fig 3. Dorsoventral projection of a 2 year old *Saimiri boliviensis peruviansis*. The cardio-thoracic ratio is shown with the black lines; The left and right costophrenic angles are visualized with the white lines where the diaphragm meets the ribs. Note the presence of a clavicle (white arrow).

<https://doi.org/10.1371/journal.pone.0201646.g003>

- The costophrenic angles were measured on the right (RCA) and left side (LCA) on the DV projection and were defined where the diaphragm meets the ribs [30] (Fig 3).
- The major vessels diameter refers to aorta (AO) diameter and caudal vena cava (CVC) diameter on a lateral projection (Fig 1). The projection was chosen where the edges of the vessel were better visualized. We assumed that the diameter would not change significantly from one lateral to another giving the small size of the patient. The ratio CVC/AO was measured as published in dogs [39].
- The ratio between the width of the thoracic vertebrae and cranial mediastinum has been recorded on the DV projection (Fig 3).

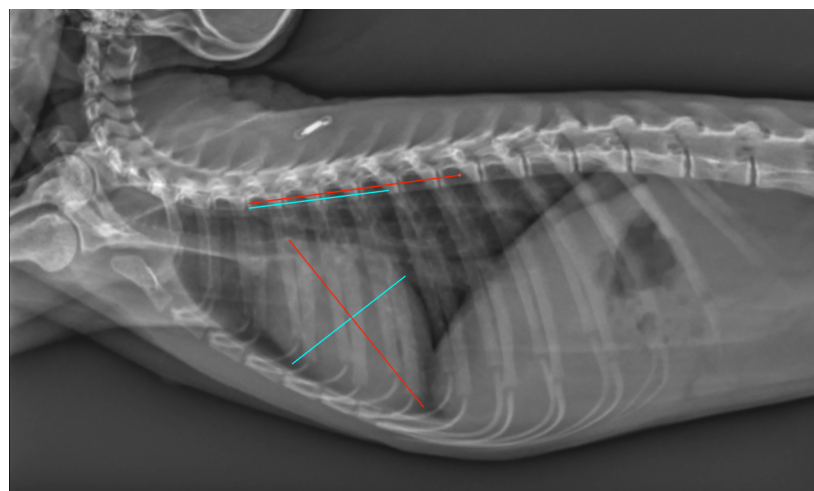


Fig 4. Left-right lateral thoracic radiograph of a 4y old female *Saimiri boliviensis peruviansis* illustrating the measurement of the VHS (Vertebral Heart Score).

<https://doi.org/10.1371/journal.pone.0201646.g004>

Results

Relevant skeletal system

All the animal had 13 thoracic vertebrae with presence of 13 pair of ribs and two pairs (12/13 animals) or one pair (1/13) of floating ribs. One male demonstrated an elongated transverse process of L1 on the right side. The caudal thoracic vertebral bodies demonstrated larger length and width compared to the cranial thoracic vertebral bodies (Fig 5) as published in ver-vet monkeys [29]. The anticlinal vertebra was always T11 as in most dogs [40].

An average of 7,23 sternebrae (range: 6–8) were present in all the monkeys, including the manubrium and xyphoid. The average of the length and width of the third sternebrae were $5,72 \text{ mm} \pm 0,86 \text{ mm}$ (range: 4,18–6,86 mm) and $2,2 \text{ mm} \pm 0,35 \text{ mm}$ (range: 1,78–2,82 mm) respectively. The values were measured on the third sternebrae because it was better visualized on all the examinations.

The clavicae were present in all the 13 monkeys (Fig 3).

All the radiographic findings of the skeletal system are summarized in Table 1.

Cardio-vascular system

Left-right lateral (RL) projection. The length of the long axis (height) and short axis (width) of the cardiac silhouette on the RL projection were $2,95 \pm 0,23 \text{ cm}$ (range: 2,54–3,32) and $2,05 \pm 0,12 \text{ cm}$ (range: 1,86–2,29) respectively. The mean RL-VHS was $8,98 \pm 0,25$ (range: 8,5–9,3). The cardio thoracic ratio was $0,76 \pm 0,04$ (range: 0,69–0,82). The number of intercostal spaces occupied by the cardiac silhouette was $3,08 \pm 0,34$ (range: 2,5–3,5 spaces). The number of sternebrae in contact with the cardiac silhouette was $3,08 \pm 0,19$ (range: 3–3,5 sternebrae). The angle of cardiac inclination was $35,43^\circ \pm 7,06^\circ$ (range: 25,5–46,01).

Right-left lateral (LL) projection. The height and width of the cardiac silhouette were $2,81 \pm 0,16 \text{ cm}$ (range: 2,52–3,05) and $2,13 \pm 0,18 \text{ cm}$ (range: 1,8–2,34) respectively. The mean LL-VHS was $8,85 \pm 0,35$ (range: 8,6–9,5).

Dorsoventral (DV) projection. The apex of the heart was always positioned to the left. The width of the cardiac silhouette at the widest point was $2,38 \pm 0,17 \text{ cm}$ (range: 2,05–2,74) and the thoracic width taken at the same level was $3,49 \pm 0,17 \text{ cm}$ (range: 3,29–3,9). The cardio-thoracic ratio was then $0,68 \pm 0,03$ (range: 0,61–0,71).

The radiographic findings of the cardiac system are summarized in Table 2.

The caudal vena cava was better visualized and delineated in right-left lateral projection in all patients. Compared to the caudal vena cava, the aorta was less conspicuous and the edges

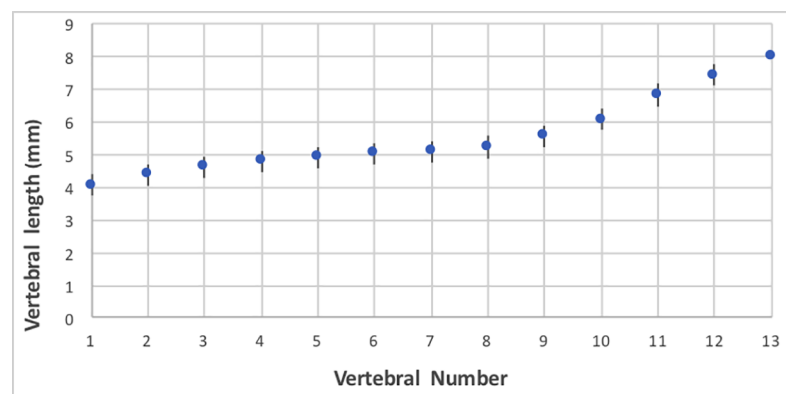


Fig 5. Means and standard deviations of radiographic vertebral body lengths in 13 *Saimiri* spp. Note the rapid increase in vertebral body length caudal to T9.

<https://doi.org/10.1371/journal.pone.0201646.g005>

Table 1. Summarized radiographic measurements (mm) and findings of the skeletal system of 13 healthy anesthetized *Saimiri* spp.

	Variables	Mean ± SD	Range (min-max)
T1	Length	4,07 ± 0,36	3,6–4,86
	Height	2,08±0,23	1,46–2,43
T2	Length	4,39 ± 0,32	3,92–5,06
	Height	2,17±0,17	1,96–2,53
T3	Length	4,62 ± 0,37	3,91–5,11
	Height	2,30±0,23	2,05–2,73
T4	Length	4,79 ± 0,31	4,04–5,32
	Height	2,26±0,29	1,95–2,92
T5	Length	4,91 ± 0,34	4,22–5,47
	Height	2,26±0,29	1,95–2,92
T6	Length	5,02 ± 0,36	4,3–5,62
	Height	2,60±0,33	2,11–3,14
T7	Length	5,09 ± 0,36	4,3–5,59
	Height	2,77±0,35	2,18–3,34
T8	Length	5,23 ± 0,35	4,76–6,04
	Height	2,82±0,36	2,09–3,38
T9	Length	5,55 ± 0,30	4,53–5,32
	Height	3,02±0,29	2,65–3,44
T10	Length	6,06 ± 0,29	5,66–6,59
	Height	3,17±0,37	2,72–3,94
T11	Length	6,82 ± 0,36	6,33–7,48
	Height	3,28 ± 0,40	2,61–3,91
T12	Length	7,43 ± 0,38	6,75–8,22
	Height	3,31 ± 0,39	2,57–3,91
T13	Length	8,02 ± 0,22	7,36–9,06
	Height	3,54 ± 0,33	2,88–3,91
Anticlinal vertebrae		11	
St 3	Length	5,72±0,86	4,18–6,86
	Height	2,2±0,35	1,78–2,82
Number of St		7,23 ± 0,73	6–8
Number of ribs	Total		13
	Floating		1–2

T: Thoracic vertebrae. St: Sternebrae.

<https://doi.org/10.1371/journal.pone.0201646.t001>

were less clear in all patients. The mean aortic diameter was 4,14 mm ± 0,36 mm and caudal vena cava was 4,47 mm ± 0,36 mm with the ratio CVC/AO at 1,08 ± 0,09 (range: 0,91–1,20) (Table 3). The pulmonary vessels were mildly visualized in 10/13 animals and barely visible in 3/13 animals. As for the major vessels, the pulmonary vessels were better visualized in right-left lateral projection.

Respiratory system

Overall, a mild diffuse interstitial pattern was noted in 8/13 monkeys, independently of the body condition and the age. On the left-right lateral radiograph, the tip of the lung lobes ended at T11 (1/13), T12 (5/13), T13 (6/13) and L1 for 1/13 patients. On the DV projection the diaphragm ended at the level of T9 (8/13) or T10 (5/13) and the right and left costophrenic angles were respectively 33,01° ± 5,29° and 34,40° ± 7,11°.

Table 2. Radiographic findings (cm) of the cardiac system of healthy anesthetized *Saimiri* spp.

	Projection	Variables	Mean ± SD	Range (min-max)
Cardiac silhouette	RL	Height	2,95 ± 0,23	2,54–3,32
		Width	2,05 ± 0,12	1,86–2,86
VHS		8,98 ± 0,25	8,5–9,3	
Thoracic size		Height	3,89 ± 0,31	3,36–4,32
Cardio-thoracic ratio			0,76 ± 0,04	0,69–0,82
Number of intercostal spaces			3,08 ± 0,34	2,5–3,5
Number of sternbrae in contact			3,08 ± 0,19	3–3,5
Angle of cardiac inclination			35,43 ± 7,06	25,5–46,01
Cardiac silhouette	LL	Height	2,81 ± 0,16	2,52–3,05
		Width	2,13 ± 0,18	1,8–2,34
VHS		8,85 ± 0,35	8,6–9,5	
Cardiac size	DV	Width	2,38 ± 0,17	2,05–2,74
Thoracic size		Width	3,49 ± 0,17	3,29–3,9
Cardio-thoracic ratio			0,68 ± 0,03	0,61–0,71

VHS: Vertebral Heart Score, RL: left-right Lateral, LL: right-left Lateral, DV: dorsoventral

<https://doi.org/10.1371/journal.pone.0201646.t002>

In all the 13 monkeys, the tracheal rings were mineralized and the trachea was well visualized. The carina was seen at the level of the third intercostal space (10/13) or at the level of the fourth intercostal space (3/13). On the DV projection, the trachea was not consistently visualized and often superimposed with the vertebral bodies. The trachea to inlet ratio was $0,33 \pm 0,04$ (Table 4). The tracheal inclination was ranged between $10,04^\circ$ and $19,7^\circ$ with an average at $14,62^\circ \pm 3,44^\circ$. The radiographic findings for the respiratory system are summarized in the Table 4.

Discussion

A lot of characteristics make the squirrel monkey pertinent to research. Furthermore, many studies have been conducted in order improve the conservation of different subspecies of *Saimiri* spp. [41–43]. This study provides the first thoracic radiography data from anesthetized clinically healthy male and female squirrel monkeys and provides new references ranges. These indices are helpful in diagnosing respiratory and cardiovascular disorders and characterizing these disease processes in animal disease models [27]. The integrated readout system allows a faster image acquisition and images are directly sent to computer. In this case, the post processing of the images is very important due to the small size of the patient and non-optimal window and level. The DV projection was also chosen instead of VD because of the flat chest conformation of the patient; the DV was straighter and subjectively more repeatable. The neck was extended as much as possible on the DV projection.

Primates have different number of thoracic vertebrae depending on the species. The thoracic region is more variable compared to the cervical or lumbar, with the number of vertebrae

Table 3. Radiographic anatomical measurements of the main vascular structures (mm).

	Mean ± SD	Range (min-max)
Diameter AO	4,14 ± 0,36	3,36–5,01
Diameter CVC	4,47 ± 0,36	3,90–4,82
Ratio CVC/AO	1,08 ± 0,09	0,91–1,20

<https://doi.org/10.1371/journal.pone.0201646.t003>

Table 4. Radiographic findings and measurements of the respiratory system. RCA: Right costophrenic angle, LCA: Left costophrenic angle.

	Mean ± SD	Range (min-max)
RCA	33,01 ± 5,29	27,39–42,94
LCA	34,40 ± 7,11	25,34–48,27
Trachea/thoracic inlet ratio	0,33 ± 0,04	0,24–0,37
Tracheal inclination	14,62 ± 3,44	10,04–19,7

<https://doi.org/10.1371/journal.pone.0201646.t004>

varying between 11 to 14 [44]. In the present study, all the *Saimiri* spp. had 13 pairs of ribs, with 1 or 2 pairs of floating ribs. The gradual increase in caudal thoracic vertebrae has been reported previously in primates [29], and the rate of increase varies between species [45]. This difference could be significant in some measurements, as for the VHS. However, the vertebral length remained fairly constant between T4 and T9, where the normal VHS is measured. But the accuracy of the measurement should be studied in order to precise if this difference in vertebral length could affect the VHS in a monkey with cardiac disease for example.

A mild diffuse interstitial pattern was noted in a majority of *Saimiri* spp. This pattern is considered normal in some primates [29, 46]. Although all the projections were meant to be in inspiration, it was not always feasible due to the small size of the *Saimiri* spp. This factor could also partially explain the lung pattern and affects the location of the tip of the lungs. No signs of persisting atelectasis were otherwise reported as in other monkeys [29].

A positive pressure ventilation could not be applied because the animals were not intubated. Even if this is not ideal for the examination in inspiration, it had numerous advantages. Multiple drugs have been studied in primates demonstrating their effects on the cardiovascular system [47–49]. For example, in small primates, it was demonstrated that multiple anesthetic protocols resulted in increased blood pressure and heart rate, and the isoflurane protocol showed lower value of blood pressure compared to all other protocols [50]. Using only isoflurane allows to be closer to physiological circumstances and has been indicated for debilitated animals and prolonged procedures in squirrel monkey [2]. This finding is very important, especially for the cardiovascular system. In our case, the heart rate, respiratory rate and expired CO₂ concentration were continuously monitored with pulse oxymetry present on the hand. The constant choice of the anesthetic protocol is important for the reproducibility of the results. The main problem encountered during anesthesia was hypothermia. Small body size, low body fat and long extremities contribute to rapid heat loss when these animals are anesthetized [2]. For this study, we used a heating pad, latex gloves filled with hot water and blankets. The temperature was also recorded during the entire anesthesia with a rectal probe connected directly to the anesthetic machine. The time of anesthesia was as short as possible, in order to decrease the anesthetic risk. The mean time for the three projections was 5 minutes with the total anesthetic time being 31 min ± 3,9 min (range: 22–35 min). The remaining time was used for the ECG recording and complete echocardiography. All the recoveries were smooth and without incidents.

The edges of the aorta were not always well visualized due to the superimposition of the pulmonary vessels and the interstitial pattern. However, a mean ratio with the diameter of the caudal vena cava could be calculated from the right or left lateral projection. In the present study, we assumed that the diameter would not change significantly from one lateral projection to another due to the small size of the patient. The projection was chosen in function of the good visualization of the edges. The ratio CVC/AO may be a useful tool for the diagnosis of right-sided cardiac failure in dogs [39]. The normal ratio can therefore give a reference value, but further studies have to be done in animals with right-sided heart disease. The

pulmonary vessels were smaller and no definitive ratio with the ribs, as in dogs, could be presented.

The vertebral heart score was also calculated on the two lateral projections. In dogs, the RL-VHS is significantly higher compared to LL-VHS [51]. This is supposed to be a consequence of the magnification. In the present study, the RL-VHS was also mildly higher compared to LL-VHS but the small size made this difference insignificant. The other measurements were calculated from the RL projection because this is the most used lateral projection. The number of sternbrae in contact with the cardiac silhouette is also a useful tool as it can be increased in case of cardiomegaly [52]. Other measurements that could help in case of suspicion of cardiomegaly are for example dorsal deviation of the trachea with narrowing of the tracheal inclination [40].

The measurements are assumed to give reference ranges for healthy animals based on the following criteria: normal general behavior and physical examination, all the echocardiographic measurements were within available normal reference ranges as previously published [23], and normal cardiac troponin I values [53]. Cardiomyopathy and heart failure are the primary health concern in the geriatric *Saimiri* spp. population [23], and more precisely HCM or DCM [11, 16]. The cardiac silhouette in these cases would appear enlarged, as a left sided or generalized cardiomegaly (increased VHS, elevation of the trachea, elongation of the left ventricle, rounding of the left heart border) [40]. Secondary signs of left-sided congestive cardiac failure (venous congestion and increased lung pattern) or right-sided congestive heart failure (hepatomegaly, CVC congestion and suspicion of ascites in the cranial abdomen included) can also be present.

Limitations

There are several limitations in this study.

The small number of patients is the first limitation. There were a lot of variations in the age and weights. The low number of patients does not allow to assess statistical differences between different measurements, as for changes in cardiac size with age, cardiac inclination and shape. In cats, the cardiac size is proven to be larger in young cat, and more tortuous (tortuous aortic arch) with a pronounced cardiac inclination in aged cats for example [52]. No sex differences could be proven as well. Other studies have to be done with a larger group and a differentiation between male/female and also young/older animals.

In conclusion, knowing the normal measurements of thoracic radiographic parameters is essential for defining abnormalities. This study gives an overview of normal thoracic radiographic anatomy and gives primary reference values in *Saimiri* spp. monkeys. These findings are useful in veterinary medicine practice as well as in research involving non-human primate models of respiratory or cardiovascular disorders and morphologic studies on squirrel monkeys (*Saimiri* spp.).

Supporting information

S1 Fig. Left-right lateral projection of a 9 years old *Saimiri sciureus*. Size of the thoracic vertebrae, sternbrae, diameter of the aorta, caudal vena cava and angle of cardiac inclination can be measured.

(TIF)

S2 Fig. Right-left lateral projection of a 4 year old *Saimiri boliviensis peruviansis*. Tracheal diameter to thoracic inlet length ratio and tracheal inclination can be measured.

(TIF)

S3 Fig. Dorsoventral projection of a 2 year old *Saimiri boliviensis peruviansis*. The cardiothoracic, left and right costophrenic angles are measured. Note the presence of a clavícula. (TIF)

S4 Fig. Left-right lateral thoracic radiograph of a 4y old female *Saimiri boliviensis peruviansis*. Measurement of the VHS (Vertebral Heart Score). (TIF)

S1 Supporting Information. *Saimiri* spp. xlsx. Informations concerning the animals. (XLSX)

S2 Supporting Information. Raw data *Saimiri* spp. Xray.xlsx. Raw data of all 13 animals. (XLSX)

Acknowledgments

The authors would like to thank the Zoo of Pairi Daiza that paid for the blood sample analysis (NT-pro BNP and troponin I), provided the digital X-ray machine as well as the zoological team of Pairi Daiza for providing the facilities to conduct the study.

Author Contributions

Conceptualization: Blandine Houdellier, Pascale Smets, Jimmy H. Saunders.

Data curation: Blandine Houdellier, Véronique Liekens, Pascale Smets, Tim Bouts.

Formal analysis: Blandine Houdellier, Véronique Liekens, Pascale Smets, Tim Bouts.

Funding acquisition: Véronique Liekens, Pascale Smets, Tim Bouts.

Investigation: Véronique Liekens, Tim Bouts.

Methodology: Blandine Houdellier, Véronique Liekens, Pascale Smets, Tim Bouts.

Project administration: Blandine Houdellier, Véronique Liekens, Pascale Smets, Tim Bouts, Jimmy H. Saunders.

Resources: Tim Bouts, Jimmy H. Saunders.

Software: Tim Bouts.

Supervision: Pascale Smets, Tim Bouts.

Validation: Pascale Smets, Tim Bouts, Jimmy H. Saunders.

Writing – original draft: Blandine Houdellier.

Writing – review & editing: Véronique Liekens, Pascale Smets, Tim Bouts, Jimmy H. Saunders.

References

1. Rylands A, Mittermeier R. Family Cebidae (capuchins and squirrel monkeys). Handbook of the Mammals of the World. 2013; 3:348–89.
2. Brady AG. Research techniques for the squirrel monkey (*Saimiri* sp.). ILAR J. 2000; 41(1):10–8. PMID: [11406698](https://pubmed.ncbi.nlm.nih.gov/11406698/).
3. Lynch Alfaro JW, Boubli JP, Paim FP, Ribas CC, Silva MN, Messias MR, et al. Biogeography of squirrel monkeys (genus *Saimiri*): South-central Amazon origin and rapid pan-Amazonian diversification of a lowland primate. Mol Phylogenet Evol. 2015; 82 Pt B:436–54. <https://doi.org/10.1016/j.ympev.2014.09.004> PMID: [25305518](https://pubmed.ncbi.nlm.nih.gov/25305518/).

4. Lopez-Torres S, Schillaci MA, Silcox MT. Life history of the most complete fossil primate skeleton: exploring growth models for *Darwinius*. *R Soc Open Sci*. 2015; 2(9):150340. <https://doi.org/10.1098/rsos.150340> PMID: 26473056; PubMed Central PMCID: PMC4593690.
5. Marroig G. When size makes a difference: allometry, life-history and morphological evolution of capuchins (*Cebus*) and squirrels (*Saimiri*) monkeys (Cebinae, Platyrrhini). *BMC Evol Biol*. 2007; 7:20. Epub 2007/02/16. <https://doi.org/10.1186/1471-2148-7-20> PMID: 17300728; PubMed Central PMCID: PMC1808050.
6. Merces MP, Lynch Alfaro JW, Ferreira WA, Harada ML, Silva Junior JS. Morphology and mitochondrial phylogenetics reveal that the Amazon River separates two eastern squirrel monkey species: *Saimiri sciureus* and *S. collinsi*. *Mol Phylogenet Evol*. 2015; 82 Pt B:426–35. <https://doi.org/10.1016/j.ympev.2014.09.020> PMID: 25451802.
7. Blomquist GE, Williams LE. Quantitative genetics of costly neonatal sexual size dimorphism in squirrel monkeys (*Saimiri boliviensis*). *J Evol Biol*. 2013; 26(4):756–65. <https://doi.org/10.1111/jeb.12096> PMID: 23437981; PubMed Central PMCID: PMC4646609.
8. Young JW. Ontogeny of joint mechanics in squirrel monkeys (*Saimiri boliviensis*): functional implications for mammalian limb growth and locomotor development. *J Exp Biol*. 2009; 212(Pt 10):1576–91. <https://doi.org/10.1242/jeb.025460> PMID: 19411552; PubMed Central PMCID: PMC4677092.
9. Polgar Z, Wood L, Haskell MJ. Individual differences in zoo-housed squirrel monkeys' (*Saimiri sciureus*) reactions to visitors, research participation, and personality ratings. *Am J Primatol*. 2017. <https://doi.org/10.1002/ajp.22639> PMID: 28150428.
10. Zimble-Delorenzo HS, Stone AI. Integration of field and captive studies for understanding the behavioral ecology of the squirrel monkey (*Saimiri* sp.). *Am J Primatol*. 2011; 73(7):607–22. Epub 2011/03/16. <https://doi.org/10.1002/ajp.20946> PMID: 21404315.
11. Brady AG, Watford JW, Massey CV, Rodning KJ, Gibson SV, Williams LE, et al. Studies of heart disease and failure in aged female squirrel monkeys (*Saimiri* sp.). *Comp Med*. 2003; 53(6):657–62. PMID: 14727815.
12. Rishniw M, Schiavetta AM, Johnson TO, Erb HN. Cardiomyopathy in captive owl monkeys (*Aotus nancymae*). *Comp Med*. 2005; 55(2):162–8. PMID: 15884779.
13. Lammey ML, Lee DR, Ely JJ, Sleeper MM. Sudden cardiac death in 13 captive chimpanzees (*Pan troglodytes*). *J Med Primatol*. 2008; 37 Suppl 1:39–43. <https://doi.org/10.1111/j.1600-0684.2007.00260.x> PMID: 18269527.
14. Meehan T, Lowenstine L, editors. Causes of mortality in captive lowland gorillas: a survey of the SSP population. *Proc Am Assoc Zoo Vet Annu Meet*; 1994.
15. Nunamaker EA, Lee DR, Lammey ML. Chronic diseases in captive geriatric female Chimpanzees (*Pan troglodytes*). *Comp Med*. 2012; 62(2):131–6. PMID: 22546920; PubMed Central PMCID: PMC4318251.
16. Tolwani RJ, Waggie KS, Green SL, Tolwani AJ, Lyons DM, Schatzberg AF. Dilative cardiomyopathy leading to congestive heart failure in a male squirrel monkey (*Saimiri sciureus*). *J Med Primatol*. 2000; 29(1):42–5. PMID: 10870674.
17. Flanders JA Jr., Buoscio DA, Jacobs BA, Gamble KC. Retrospective Analysis of Adult-Onset Cardiac Disease in Francois' Langurs (*Trachypithecus francoisi*) Housed in U.S. Zoos. *J Zoo Wildl Med*. 2016; 47(3):717–30. <https://doi.org/10.1638/2015-0119.1> PMID: 27691958.
18. Baldessari A, Snyder J, Ahrens J, Murnane R. Fatal myocardial fibrosis in an aged chimpanzee (*Pan troglodytes*). *Pathobiol Aging Age Relat Dis*. 2013; 3. <https://doi.org/10.3402/pba.v3i0.21073> PMID: 23762500; PubMed Central PMCID: PMC43679521.
19. Hansen JF, Alford PL, Keeling ME. Diffuse myocardial fibrosis and congestive heart failure in an adult male chimpanzee. *Vet Pathol*. 1984; 21(5):529–31. <https://doi.org/10.1177/030098588402100514> PMID: 6485212.
20. Lammey ML, Baskin GB, Gigliotti AP, Lee DR, Ely JJ, Sleeper MM. Interstitial myocardial fibrosis in a captive chimpanzee (*Pan troglodytes*) population. *Comp Med*. 2008; 58(4):389–94. PMID: 18724782; PubMed Central PMCID: PMC43706041.
21. Schulman FY, Farb A, Virmani R, Montali RJ. Fibrosing cardiomyopathy in captive western lowland gorillas (*Gorilla gorilla gorilla*) in the United States: a retrospective study. *Journal of Zoo and Wildlife Medicine*. 1995:43–51.
22. Kanthaswamy S, Reader R, Tarara R, Oslund K, Allen M, Ng J, et al. Large scale pedigree analysis leads to evidence for founder effects of Hypertrophic Cardiomyopathy in Rhesus Macaques (*Macaca mulatta*). *J Med Primatol*. 2014; 43(4):288–91. <https://doi.org/10.1111/jmp.12127> PMID: 25422529; PubMed Central PMCID: PMC4240635.

23. Huss MK, Ikeno F, Buckmaster CL, Albertelli MA. Echocardiographic and electrocardiographic characteristics of male and female squirrel monkeys (*Saimiri* spp.). *J Am Assoc Lab Anim Sci*. 2015; 54(1):25–8. PMID: [25651087](#); PubMed Central PMCID: PMC4311738.
24. Makungu M, du Plessis WM, Barrows M, Groenewald HB, Koeppel KN. Radiographic thoracic anatomy of the ring-tailed lemur (*Lemur catta*). *J Med Primatol*. 2014; 43(3):144–52. <https://doi.org/10.1111/jmp.12102> PMID: [24444331](#).
25. Kubiak ML, Jayson SL, Saunders RA. Determination of vertebral heart score in Goeldi's monkeys (*Callimico goeldii*). *J Med Primatol*. 2015; 44(4):183–6. <https://doi.org/10.1111/jmp.12173> PMID: [25912407](#).
26. Ji Y, Xie L, Liu S, Cheng K, Xu F, Li X, et al. Correlation of thoracic radiograph measurements with age in adolescent Chinese rhesus macaques (*Macaca mulatta*). *J Am Assoc Lab Anim Sci*. 2013; 52(1):78–82. PMID: [23562037](#); PubMed Central PMCID: PMC3548205.
27. Xie L, Zhou Q, Liu S, Wu Q, Ji Y, Zhang L, et al. Normal thoracic radiographic appearance of the cynomolgus monkey (*Macaca fascicularis*). *PLoS One*. 2014; 9(1):e84599. <https://doi.org/10.1371/journal.pone.0084599> PMID: [24416248](#); PubMed Central PMCID: PMC3885584.
28. Schillaci MA, Jones-Engel L, Heidrich JE, Benamore R, Pereira A, Paul N. Thoracic radiography of pet macaques in Sulawesi, Indonesia. *J Med Primatol*. 2008; 37(3):141–5. <https://doi.org/10.1111/j.1600-0684.2007.00250.x> PMID: [18547258](#).
29. Young AN, du Plessis WM, Rodriguez D, Beierschmitt A. Thoracic radiographic anatomy in vervet monkeys (*Chlorocebus sabaeus*). *J Med Primatol*. 2013; 42(6):310–7. <https://doi.org/10.1111/jmp.12058> PMID: [23848259](#).
30. Alves FR, Costa FB, Machado PP, Diniz AdN, Araújo AVC, Ambrósio CE, et al. Anatomical and radiographic appearance of the capuchin monkey thoracic cavity (*Cebus apella*). *Pesquisa Veterinária Brasileira*. 2012; 32:1345–50.
31. Pinheiro LL, Lima AR, Muniz JA, Imbeloni A, Fioreto ET, Fontes RF, et al. Anatomy and morphometric aspects of the trachea of *Saimiri sciureus* Linnaeus, 1758: knowledge for emergency procedures. *An Acad Bras Cienc*. 2012; 84(4):973–7. PMID: [23207702](#).
32. Szentiks CA, Kondgen S, Silinski S, Speck S, Leendertz FH. Lethal pneumonia in a captive juvenile chimpanzee (*Pan troglodytes*) due to human-transmitted human respiratory syncytial virus (HRSV) and infection with *Streptococcus pneumoniae*. *J Med Primatol*. 2009; 38(4):236–40. <https://doi.org/10.1111/j.1600-0684.2009.00346.x> PMID: [19239572](#).
33. Carne B, Ajzenberg D, Demar M, Simon S, Dardé ML, Maubert B, et al. Outbreaks of toxoplasmosis in a captive breeding colony of squirrel monkeys. *Veterinary parasitology*. 2009; 163(1):132–5.
34. Cedillo-Peláez C, Rico-Torres CP, Salas-Garrido CG, Correa D. Acute toxoplasmosis in squirrel monkeys (*Saimiri sciureus*) in Mexico. *Veterinary parasitology*. 2011; 180(3):368–71.
35. Padovan D, Cantrell C. Causes of death of infant rhesus and squirrel monkeys. *J Am Vet Med Assoc*. 1983; 183(11):1182–4. PMID: [6643230](#).
36. Dennis R. *Handbook of small animal radiology and ultrasound*: Churchill Livingstone/Elsevier; 2010.
37. Moon M, Keene BW, Lessard P, Lee J. Age related changes in the feline cardiac silhouette. *Veterinary Radiology & Ultrasound*. 1993; 34(5):315–20.
38. Buchanan JW, Bucheler J. Vertebral scale system to measure canine heart size in radiographs. *J Am Vet Med Assoc*. 1995; 206(2):194–9. PMID: [7751220](#).
39. Lehmkuhl LB, Bonagura JD, Biller DS, Hartman WM. Radiographic evaluation of caudal vena cava size in dogs. *Veterinary radiology & ultrasound: the official journal of the American College of Veterinary Radiology and the International Veterinary Radiology Association*. 1997; 38(2):94–100. PMID: [9238776](#).
40. Thrall DE. *Textbook of veterinary diagnostic radiology*: Elsevier Health Sciences; 2013.
41. Denis LT, Poindexter AN, Ritter MB, Seager SWJ, Deter RL. Freeze Preservation of Squirrel Monkey Sperm for Use in Timed Fertilization Studies*. *Fertility and Sterility*. 1976; 27(6):723–9. [http://dx.doi.org/10.1016/S0015-0282\(16\)41905-9](http://dx.doi.org/10.1016/S0015-0282(16)41905-9). PMID: [819313](#)
42. Oliveira KG, Leão DL, Almeida DVC, Santos RR, Domingues SFS. Seminal characteristics and cryopreservation of sperm from the squirrel monkey, *Saimiri collinsi*. *Theriogenology*. 2015; 84(5):743–9.e1. <http://dx.doi.org/10.1016/j.theriogenology.2015.04.031>. PMID: [26047706](#)
43. Oliveira KG, Santos RR, Leao DL, Brito AB, Lima JS, Sampaio WV, et al. Cooling and freezing of sperm from captive, free-living and endangered squirrel monkey species. *Cryobiology*. 2016; 72(3):283–9. <https://doi.org/10.1016/j.cryobiol.2016.03.004> PMID: [26994833](#).
44. Angel JL, Swindler DR, Wood CD. *An Atlas of Primate Gross Anatomy*. JSTOR; 1975.
45. Ankel-Simons F. *Primate anatomy: an introduction*: Academic Press; 2010.

46. Silverman S, Morgan JP. Thoracic radiography of the normal rhesus macaque (*Macaca mulatta*). *American journal of veterinary research*. 1980; 41(10):1704–19. Epub 1980/10/01. PMID: [7224301](#).
47. Larsen RS, Moresco A, Sauther ML, Cuozzo FP. Field anesthesia of wild ring-tailed lemurs (*Lemur catta*) using tiletamine-zolazepam, medetomidine, and butorphanol. *J Zoo Wildl Med*. 2011; 42(1):75–87. <https://doi.org/10.1638/2010-0144.1> PMID: [22946374](#).
48. Larsen RS, Sauther ML, Cuozzo FP. Evaluation of modified techniques for immobilization of wild ring-tailed lemurs (*Lemur catta*). *J Zoo Wildl Med*. 2011; 42(4):623–33. <https://doi.org/10.1638/2011-0004.1> PMID: [22204057](#).
49. Tsusaki H, Yonamine H, Tamai A, Shimomoto M, Kuwano K, Iwao H, et al. Left ventricular volume and function in cynomolgus monkeys using real-time three-dimensional echocardiography. *J Med Primatol*. 2007; 36(1):39–46. <https://doi.org/10.1111/j.1600-0684.2006.00192.x> PMID: [17359465](#).
50. Chaves RH, Souza NF, Imbeloni AA, Neves AC, Teixeira RK, Santos Cde C. Evaluation of blood pressure in feline night monkeys (*Aotus azarae infulatus*) under different restraint protocols. *J Med Primatol*. 2015; 44(6):349–54. <https://doi.org/10.1111/jmp.12183> PMID: [26222788](#).
51. Greco A, Meomartino L, Raiano V, Fatone G, Brunetti A. Effect of left vs. right recumbency on the vertebral heart score in normal dogs. *Veterinary radiology & ultrasound: the official journal of the American College of Veterinary Radiology and the International Veterinary Radiology Association*. 2008; 49(5):454–5. Epub 2008/10/07. PMID: [18833953](#).
52. Guglielmini C, Diana A. Thoracic radiography in the cat: Identification of cardiomegaly and congestive heart failure. *J Vet Cardiol*. 2015; 17 Suppl 1:S87–101. <https://doi.org/10.1016/j.jvc.2015.03.005> PMID: [26776597](#).
53. Feltrer Y, Strike T, Routh A, Gaze D, Shave R. Point-of-care cardiac troponin I in non-domestic species: a feasibility study. 2016.